

## Calorimetric and FTIR Study of the Acid Properties of Sulfated Titanias

A. Desmartin-Chomel,<sup>†</sup> J. L. Flores,<sup>†</sup> A. Bourane,<sup>†</sup> J. M. Clacens,<sup>†</sup> F. Figueras,<sup>\*,‡</sup> G. Delahay,<sup>‡</sup> A. Giroir Fendler,<sup>‡</sup> and C. Lehaut-Burnouf<sup>§</sup>

*Institut de Recherches sur la Catalyse (CNRS UPR5401), 2 avenue A. Einstein, 69626 Villeurbanne, France, Laboratoire de Matériaux Catalytiques et Catalyse en Chimie Organique (UMR 5618 ENSCM-CNRS 8), Rue de l'Ecole Normale 34296 Montpellier, France, Millennium Inorganic Chemicals, Rueil, France, Laboratoire d'Application de la Chimie à l'Environnement, (UMR 5634 CNRS-UCB Lyon 1), 43, boulevard du 11 novembre 1918, 69622 Villeurbanne Cedex, France*

*Received: June 8, 2005; In Final Form: November 17, 2005*

Titanium oxides of different surface areas were sulfated then calcined to convert the solid to a strong acid. The amount of sulfur retained by the solid and the thermal stability of the resulting sulfate are controlled by the dispersion of the initial oxide. The acid properties were determined by gravimetry at 383 K, calorimetry using ammonia adsorption at 353 K, and by quantitative analysis of the infrared spectra of pyridine retained after evacuation at 423 K. A good agreement was observed between the different determinations. At low coverage of ammonia, sulfated titanias show a much lower heat of adsorption, and the IR study of NH<sub>3</sub> adsorption shows that the first doses of NH<sub>3</sub> dissociate at the surface with the formation of OH species. The lower heat of adsorption is then attributed to the contribution of NH<sub>3</sub> dissociation to the differential heat of adsorption. IR spectroscopy indicates that NH<sub>3</sub> reacts with sulfates and may lead to the transformation of disulfate species into monosulfate species on sulfated titania dioxide. A band at ca. 3574 cm<sup>-1</sup> has been assigned to  $\nu(\text{OH})$  of monosulfate species. This particular behavior makes it difficult to appreciate the initial acidity of these sulfated oxides.

### Introduction

Sulfated titanias are interesting solids that were first reported to be superacids,<sup>1</sup> with an acid strength, estimated by the adsorption of Hammett indicators, of about  $-14$ .<sup>2</sup> This acid strength, such as the catalytic activity for alkylation is lower than that of sulfated zirconias.<sup>3</sup> The titration of acid strength in liquid phase could not, however, detect sites of H<sub>0</sub> lower than  $-11.9$ .<sup>4</sup> The discrepancy can come from either differences in the procedure of titration or from different activation conditions. Indeed the number of acid sites of these solids increases with the calcination temperature up to a maximum of about 923 K then decreases.<sup>5</sup> Sulfated zirconias usually contain different forms of sulfates characterized by an infrared band at about 1395–1405 cm<sup>-1</sup> for disulfates,<sup>6–10</sup> and at 1380–1360 cm<sup>-1</sup> for sulfates. Monosulfates have been proposed to be linked to either a single Zr atom,<sup>11,12</sup> or to neighboring Zr atoms.<sup>13,14</sup> However, the investigation of sulfated tetragonal zirconias led to the assignment of the band at 1400 cm<sup>-1</sup> to a monosulfate linked to a Zr atom of high coordination, found on regular crystal planes of tetragonal ZrO<sub>2</sub>, and the band at 1380 cm<sup>-1</sup> to sulfates bound to defects.<sup>5,15,16</sup>

The interpretation of the maximum of activity as a function of calcination temperature depends, therefore, on the identification of the stronger acid sites. If it is accepted that acid sites are created by sulfates, the stronger acids have been identified to the sulfate species giving a band at 1400 cm<sup>-1</sup>. Whatever

assignment is given for this species, it corresponds to the stronger acids, since this band disappears when the solid is contacted with a weak base such as benzene.<sup>17,18</sup> It has also been recently reported that strong acidity can be introduced onto ZrO<sub>2</sub> by impregnation with disulfates.<sup>19</sup> Activation at high temperature would be required to either promote a surface reaction to form the disulfates, which do not exist initially, or to sinter the oxide in order to form the tetragonal phase. Sulfated titania has been investigated much less than the corresponding zirconia. Ammonia adsorption is commonly applied to determine the acidity of sulfated oxides,<sup>20–22</sup> and we tried to apply it to sulfated titania. However, it is also well-known that NH<sub>3</sub> is a powerful reductant, and that the acidity of sulfated zirconia is decreased by reduction.<sup>20</sup> We tried then to measure the acidity of sulfated titania using low-temperature methods, and we report, here, the results obtained using different techniques, applied to titanias of quite different surface areas.

### Experimental Section

The usual preparation procedure of TiO<sub>2</sub> involves the sulfate so that most commercial titanias are sulfated at different extents. To investigate the effect of sulfates, a gel obtained by the chloride route, which is sulfate free, was used. The original materials were titanias prepared by Millennium Inorganic Chemicals by hydrolysis of Ti sulfate (G5, DT51) or Ti chloride (GP350). Two other sulfate-free samples of lower surface area were included for comparison: P25 from Degussa, prepared by flame hydrolysis, and a rutile RL11A, supplied by Millennium. The sulfated samples were prepared from the original gel by treating with an aqueous solution (0.01, 0.1, or 1 N) of H<sub>2</sub>SO<sub>4</sub>. We suspended 5 g of solid in 100 mL of solution, left it in contact for 30 min, and then filtered, washed, and dried it at 393 K in an oven. Activation was performed by calcinations in

\* Author for correspondence: e-mail figueras@catalyse.cnrs.fr, phone 33 47244 5469, fax: 33 47244 5399.

<sup>†</sup> Institut de Recherches sur la Catalyse.

<sup>‡</sup> Laboratoire de Matériaux Catalytiques et Catalyse en Chimie Organique.

<sup>‡</sup> Millennium Inorganic Chemicals.

<sup>§</sup> Laboratoire d'Application de la Chimie à l'Environnement.

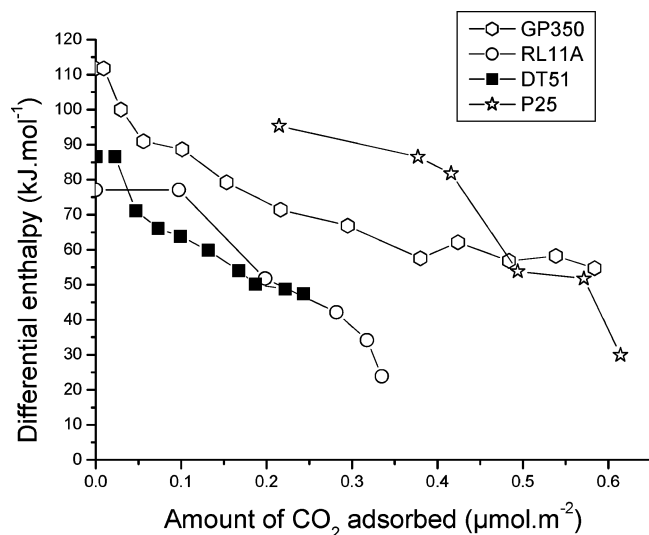


**Figure 1.** Calorimetric measurement of the adsorption of CO<sub>2</sub> on different titanias.

air at 773 K for 10 h. The denomination GP350-S1N represents a sulfated titania obtained by treating GP350 with a 1 N solution of H<sub>2</sub>SO<sub>4</sub>.

The surface areas of the solids were determined from the adsorption isotherm of N<sub>2</sub> at 77 K after standard evacuation at 523 K. The basic properties were measured by adsorption of CO<sub>2</sub> at 303 K, using a Tian-Calvet calorimeter coupled to a volumetric ramp. The samples (0.1 g) were first evacuated at 773 K, then contacted with small doses of gas, and the differential enthalpy of adsorption was measured. The acid properties were determined by adsorption of ammonia at 383 K, measured by gravimetry using a SETARAM microbalance, and then measured by calorimetry at 353 K. The results were compared to those of the adsorption of pyridine followed by FTIR, using self-supported wafers placed in glass cell, and a Bruker FTIR spectrometer. The integrated surface areas of the infrared bands obtained after desorption at 423 K were converted to milliequivalents of pyridine using the extinction coefficients reported by Rozenberg and Anderson<sup>23</sup> for sulfated oxides. The adsorption of NH<sub>3</sub> was followed by IR spectroscopy on GP350 and GP350-S-1N. The latter was preheated for 12 h under air and then for 2 h under vacuum at 473 K; nevertheless, it was not completely dehydroxylated. The former was first calcined at 773K, then recalcined at 473K under air for 12 h followed by a pretreatment under vacuum for 2 h. For IR analysis, the adsorption of NH<sub>3</sub> was performed at room temperature using self-supported pellets of catalysts.

## Results

**(1) Basicities of the Original Samples.** The thermograms of the original supports for the adsorption of CO<sub>2</sub> are reported in Figure 1, for GP350, P25, DT51, and RL11A. The results show a surface heterogeneity expected for the adsorption on oxides.

**(2) Sulfation of GP350 and P25.** By treating GP350 and P25 with solutions of increasing concentration in sulfuric acid, anionic exchange occurs and the amount of S retained before pre-treatment increases with the normality of the solution (Figure 2).

The structure of the sulfates was followed by infrared study of the band at 1350–1400 cm<sup>-1</sup> formed after vacuum treatment at 773 K. As illustrated in Figure 3, the band is broad and contains a shoulder at about 1400 cm<sup>-1</sup> on GP350-S1N and G5-S1N, which is not observed on sulfated P25 (Figure 4). The stability of sulfates was also investigated and was found to vary with the original oxide, in particular the characteristic band at

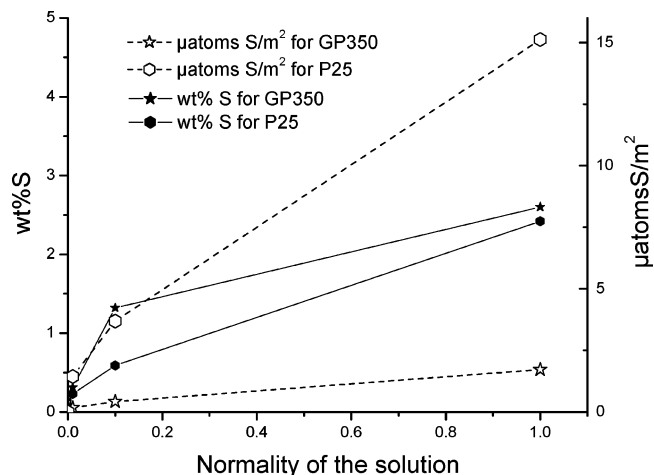


**Figure 2.** Amount of sulfur retained by the solid as a function of the normality of the solution of sulfuric acid used for anion exchange.

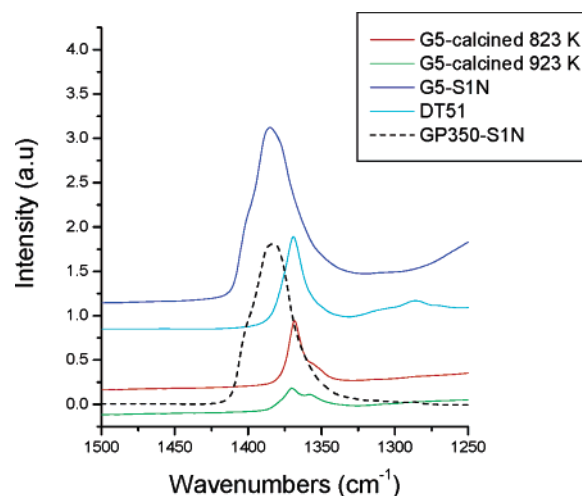


**Figure 3.** Infrared bands of sulfates for selected samples.

1370 cm<sup>-1</sup> was still observed on G5-S1N after calcination at 923 K (Figure 3), but it disappeared by evacuation of P25-S1N at about 673 K (Figure 4). The shape of the band related to sulfates also depends of the S content of the solid (Figure 5), by increasing the S loading of GP350, the intensity of the band increases as expected, but the band is displaced to higher wavenumbers with the appearance of a shoulder at 1400 cm<sup>-1</sup>.

**(3) Acidity Measurements.** Acidities were measured by several techniques, but to avoid a possible reduction of the surface by NH<sub>3</sub>, all were operated at low temperature. The results obtained are reported in Table 2, which compares the adsorption of NH<sub>3</sub> using gravimetry or calorimetry and the infrared absorption of pyridine. The two techniques of ammonia adsorption agree well on the number of sites, and the slightly lower number of acid sites measured when using pyridine is consistent with its lower basicity compared to NH<sub>3</sub>.

Here both GP350 and P25 are considered practically sulfur-free. It can be noticed that the number of acid sites created by sulfation depends on the surface area of the original titania, whereas the number of sites is doubled on GP350, it shows a modest increase on P25 (Table 1). This effect is also noticed on the density.

The strength of acid sites can be determined by calorimetry from the heat of adsorption of ammonia. The thermograms obtained for the adsorption of NH<sub>3</sub> are reported in Figure 6 for GP350 and Figure 7 for two sulfated titanias. GP350 exhibits the thermogram expected for an homogeneous surface, with a

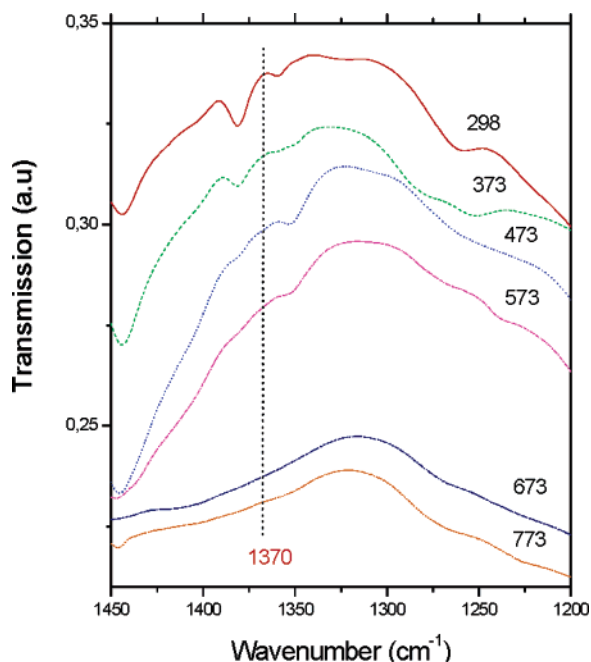


**Figure 4.** Evolution of the FTIR band of sulfates by evacuation of sulfated P25 [P25-S1N] at different temperatures.

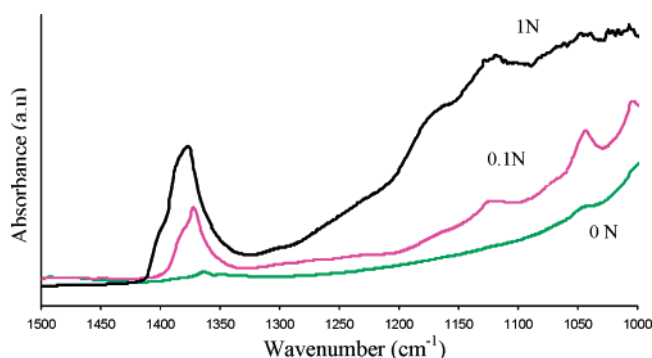


**Figure 5.** FTIR band of sulfates for the original GP350 and for the solids, obtained by treating with 0.1 and 1 N solutions of H<sub>2</sub>SO<sub>4</sub>.

relatively high initial enthalpy of 150 kJ·mol<sup>-1</sup> (Figure 6). By contrast, for sulfated samples, an initial low heat of adsorption is noticed for the first two increments, followed by an increase to a high heat of adsorption, corresponding to what is expected for a strong acid. This phenomenon is independent of the origin of titania, and is also observed on sulfated P25, but is more marked on sulfated GP350.

**(4) NH<sub>3</sub> Adsorption on Sulfated Titania Followed by FTIR.** The adsorption of NH<sub>3</sub> was investigated by FTIR on GP350 and GP350-S1N, adding small aliquots, as used in cal-

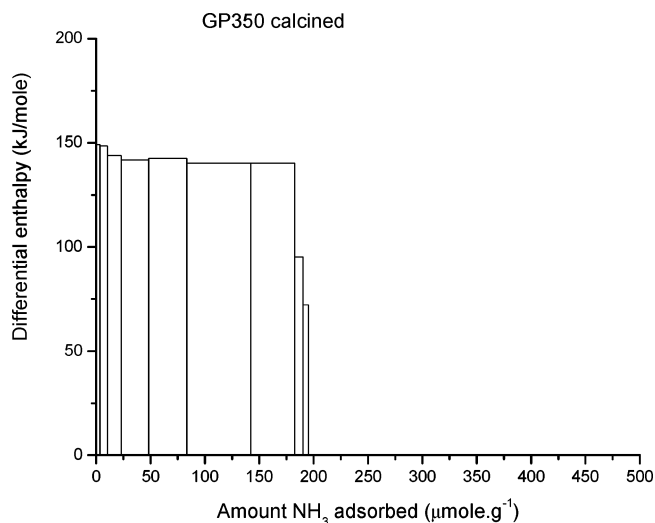


**Figure 6.** Calorimetric study of the adsorption of NH<sub>3</sub> by GP350 calcined at 823 K.

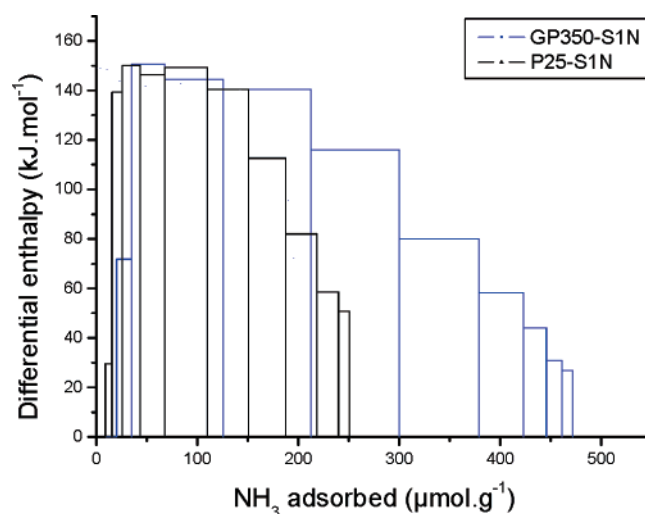


**Figure 7.** Differential heats of adsorption of ammonia on sulfated titanias.

orimetry. The IR spectra for GP350-S1N, presented in Figures 8–10, show the presence of sulfate species, characterized by the  $\nu(\text{S}=\text{O})$  at ca. 1382 cm<sup>-1</sup> (Figure 8).<sup>6, 10</sup> In the -OH region (Figure 9), the vibration at ca. 3640 cm<sup>-1</sup>, present in the starting material, has been assigned to an acidic OH linked to disulfate species for sulfated zirconia.<sup>10</sup> In presence of the five first aliquots of NH<sub>3</sub>, this band shifts slightly to 3652 cm<sup>-1</sup>, and water appears in parallel, characterized by the  $\delta(\text{H}_2\text{O})$  vibration at ca. 1600 cm<sup>-1</sup> and a broad band at ca. 3300 cm<sup>-1</sup>, assigned to  $\nu(\text{OH})$ ; other bands appear at ca. 3263, 3352, and 3388 cm<sup>-1</sup>,

**TABLE 1: Characteristics of the Titanias Used in This Work**

sample	wt % S	$S_{\text{BET}}$ (m <sup>2</sup> ·g <sup>-1</sup> )			$Q_{\text{NH}_3}$ (mmol·g <sub>cat</sub> <sup>-1</sup> )	$Q_{\text{NH}_3}$ μmol·m <sup>-2</sup>
		523 K	773K	873K		
GP350	0	220	50	45	0.32	6.40
GP350-S0.1N	0.58		69		0.30	4.35
GP350-S1N	1.3		91	57	0.74	8.13
G5	0.2	152	63		0.36	5.71
G5-S1N	2.37		100		0.40	4.00
DT51	0.56	94	74		0.23	3.11
DT51-S0.1N	1.08		74		0.26	3.51
DT51-S1N	2.44		80		0.30	3.75
P25	-	50	55		0.23	4.18
P25-S1N	0.93		50		0.26	5.20
RL11A	-	11				

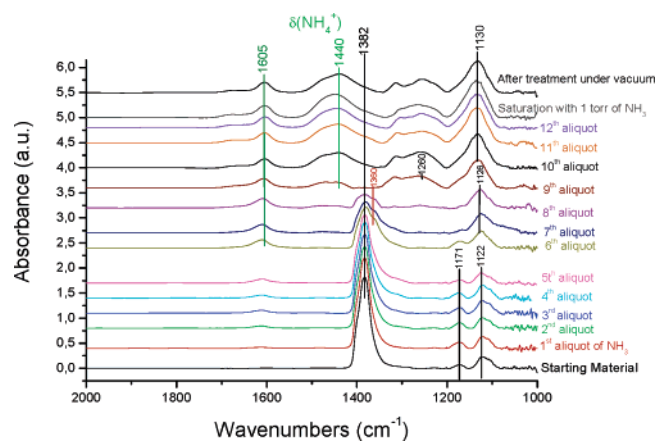


**Figure 8.** Infrared spectra showing the effect of aliquots addition of  $\text{NH}_3$  on GP350-S1N, in the spectroscopic range  $1000\text{--}2000\text{ cm}^{-1}$ .

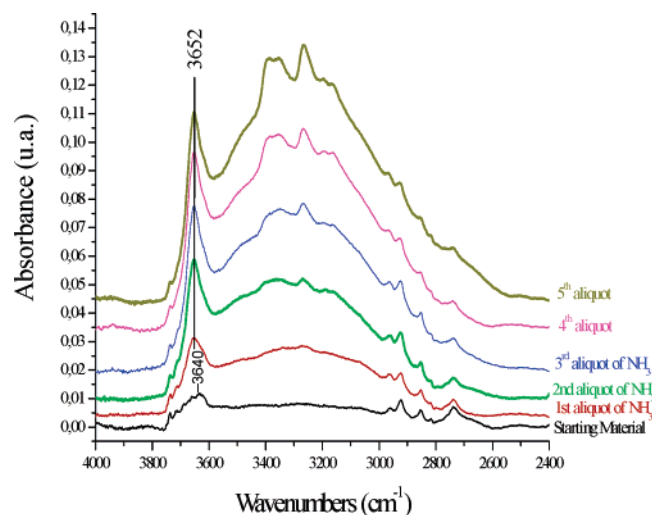


**Figure 9.** Infrared spectra showing the effect of the five first aliquots addition of  $\text{NH}_3$  on GP350-S1N, in the spectroscopic region between  $2400\text{ and }4000\text{ cm}^{-1}$ .

**TABLE 2: Acidities Measured by Different Techniques**

sample	$Q_{\text{NH}_3}$ (mmol/g <sub>cat</sub> )		$Q_{\text{py}}$ (mmol/g <sub>cat</sub> )
	ATG	calorimetry	IRTF
GP350	0.32	0.21	0.14
GP350-S0.1N	0.30		0.19
GP350-S1N	0.74	0.72	0.45
G5	0.36	0.31	0.21
G5-S1N	0.40	0.41	0.59
DT51	0.23		0.20
DT51-S0.1N	0.26		0.33
DT51-S1N	0.30		0.40
P25	0.23		0.13
P25-S1N	0.26		0.24

assigned to  $\nu(\text{N-H})$ . The formation, at low temperature, of  $-\text{OH}$  on a surface originally partially dehydroxylated is surprising, but  $\text{NH}_3$  dissociation has been reported to occur in similar conditions on titanias<sup>24</sup> and pillared clays.<sup>25</sup> Moreover, in parallel to the formation of water, the  $\nu(\text{OH})$  associated to disulfates, at ca.  $3650\text{ cm}^{-1}$ , increases in intensity from the first aliquot of  $\text{NH}_3$ . The  $\text{NH}_2$  species, expected to show bending modes around  $1500\text{ cm}^{-1}$ , were, however, not observed, probably due to a very small coverage. The dissociation of  $\text{NH}_3$  consumes energy and could account for the observed low initial enthalpy of adsorption since the overall process could be weakly exothermic.

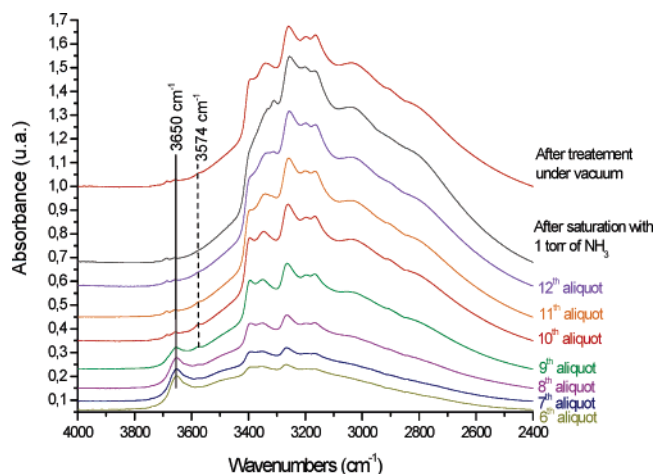


**Figure 10.** Infrared spectra showing the effect of the remaining aliquots addition of  $\text{NH}_3$  on GP350-S1N, in the spectroscopic region between  $2400\text{ and }4000\text{ cm}^{-1}$ .

After the fifth aliquot of  $\text{NH}_3$ , the sulfate band decreased in intensity because the charge of the  $\text{S=O}$  is then affected by the donation from ammonia.<sup>26</sup> This intensity decrease is coupled with the splitting of the  $\nu(\text{S=O})$  vibration and the appearance of a shoulder at ca.  $1360\text{ cm}^{-1}$  (sixth aliquot). Then the  $\nu(\text{S=O})$  vibration disappears after the eighth aliquot, and a new band appears at ca.  $1130\text{ cm}^{-1}$ , assigned to monosulfate species.<sup>27,28</sup> As observed for benzene adsorption,<sup>17</sup> the stronger acids react with  $\text{NH}_3$ , leading to their transformation and to the appearance of weaker acid sites. The disappearance of the  $\nu(\text{S=O})$  vibration is paralleled by the progressive disappearance of  $\nu(\text{OH})$  vibration at  $3650\text{ cm}^{-1}$ , associated with disulfate species.<sup>6</sup> Nevertheless, after the quasi disappearance of the  $3650\text{ cm}^{-1}$  band at the ninth aliquot, new bands appear at ca.  $3050$  and  $3200\text{ cm}^{-1}$ , and the broad band centered at ca.  $3300\text{ cm}^{-1}$  progressively increases in intensity (Figure 10). We assign this latter band to  $\nu(\text{NH}_4^+)$  of an ammonium salt.<sup>29</sup> It can be assumed that the stronger Brönsted acid sites associated with the  $3650\text{ cm}^{-1}$  band are affected by  $\text{NH}_3$ , and shifted to lower wavenumbers, due to the formation of hydrogen bonds between ammonia and OH groups. The shift of  $\nu(\text{OH})$  observed during the adsorption of benzene is up to  $200\text{ cm}^{-1}$ ,<sup>17</sup> and a much higher value is expected for a strong base as  $\text{NH}_3$ . It has to be noticed that a new band has appeared at ca.  $3574\text{ cm}^{-1}$ , that we assign to an hydroxyl vibration associated to the monosulfate species. It is visible from the seventh aliquot to the twelfth aliquot, then disappears after saturation with 1 Torr of  $\text{NH}_3$ , and re-appears after treatment under vacuum.

After the complete transformation of disulfates to monosulfates, we notice the presence of  $\text{NH}_3$  adsorbed on acidic sites at ca.  $1230\text{ cm}^{-1}$ ,  $1315\text{ cm}^{-1}$ ,  $1605\text{ cm}^{-1}$ , and protonated  $\text{NH}_4^+$  species at  $1440\text{ cm}^{-1}$ . Therefore, we suggest that  $\text{NH}_3$  first dissociated, then reacted with the disulfate groups; after the complete transformation of disulfates into monosulfates,  $\text{NH}_3$  is adsorbed at the  $\text{TiO}_2$  surface, as is shown by the increase of the broad band centered at ca.  $3245\text{ cm}^{-1}$  after the eighth aliquot.<sup>24</sup>

The infrared spectra obtained in the case of sulfate-free GP350 are quite different, as is shown in Figure 11. Sulfur exists only in trace amounts in the starting material ( $<200\text{ ppm}$ ), as shown by a very weak band at ca.  $1364\text{ cm}^{-1}$ , assigned to  $\nu(\text{S=O})$  of sulfates species (Figure 11). In the hydroxyls region (Figures 12 and 13), bands characteristic of  $\nu(\text{OH})$  vibrations in pure anatase<sup>30</sup> are present at  $3640$ ,  $3671$ ,  $3688$ ,  $3717$ , and  $3736\text{ cm}^{-1}$ , and there is a weak broad band at ca.  $3200\text{ cm}^{-1}$  due to  $\nu(\text{OH})$



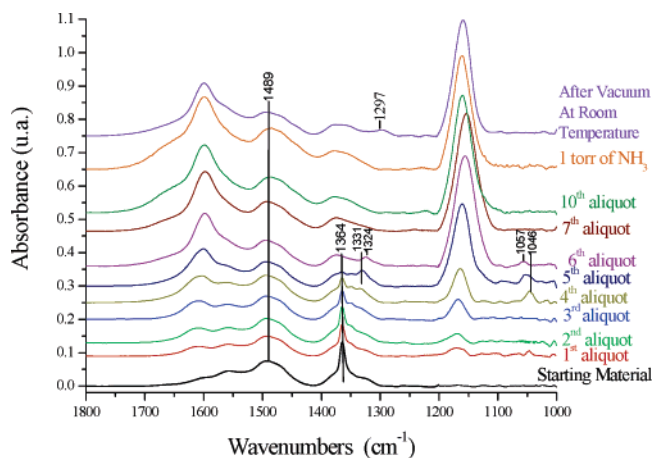


**Figure 11.** Infrared spectra showing the effect of additions of  $\text{NH}_3$  as pulses on nonsulfated GP350 in the  $\text{SO}_4$  region.

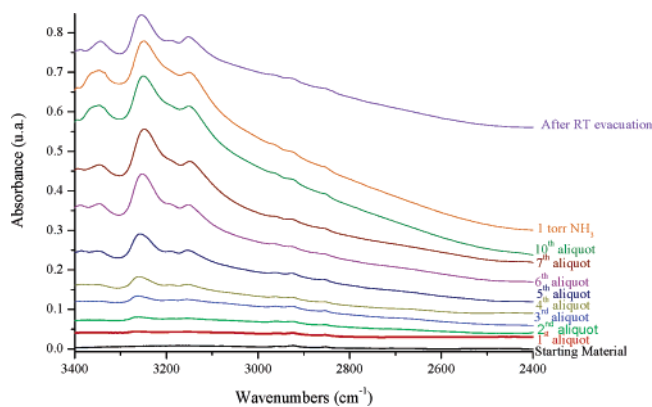


**Figure 12.** Infrared spectra showing the effect of additions of  $\text{NH}_3$  as pulses on nonsulfated GP350 in the hydroxyls region.

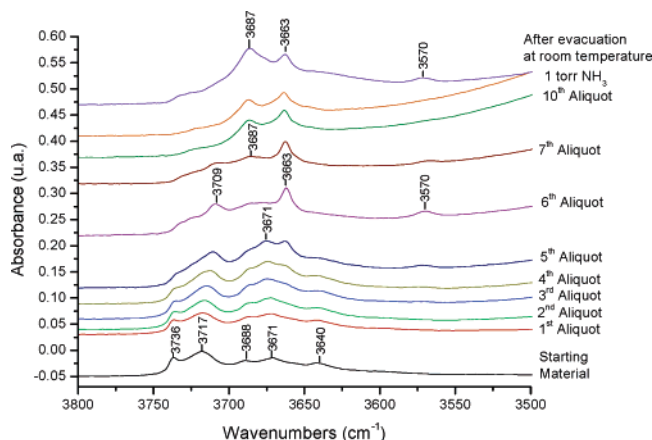


**Figure 13.** Infrared spectra showing the effect of additions of  $\text{NH}_3$  as pulses on nonsulfated GP350 in the second hydroxyls region.

of  $\text{H}_2\text{O}$ . After a few aliquots, the infrared spectra show the characteristic features of ammonia adsorbed on  $\text{TiO}_2$  with bands at ca. 1165, 1609, 3385, 3350, 3262, 3193, and 3155  $\text{cm}^{-1}$ .<sup>24,30</sup> It has to be noticed that  $\text{NH}_3$  adsorption in this case indicates, with the band at ca. 1165  $\text{cm}^{-1}$ , a weaker acid site in comparison to the GP350-S1N sample where the  $\delta(\text{NH}_3)$  vibration appears at ca. 1260  $\text{cm}^{-1}$  (Figure 8), which is characteristic of a stronger Lewis acid site. The original material contains nitrates, the band of which at 1489  $\text{cm}^{-1}$  may overlap with the bands of  $\text{NH}_4^+$  ions, expected between 1490 and 1325  $\text{cm}^{-1}$  for the deformation mode and around ca. 3000–3300  $\text{cm}^{-1}$  for  $\nu(\text{NH})$ . The constant intensity of that band at about 1489  $\text{cm}^{-1}$  would suggest however that  $\text{NH}_4^+$  are not formed. The presence of the bands

of  $\text{NH}_3$  shows the usual associative adsorption at the Lewis sites of the support, and calorimetry shows a classical behavior.

Nevertheless, upon ammonia adsorption and up to the fifth aliquot, the bands at 3736, 3688, and 3640  $\text{cm}^{-1}$  disappear, and the band at 3671  $\text{cm}^{-1}$  increases in intensity (Figure 13). From the fifth aliquot to the saturation with 1 Torr of  $\text{NH}_3$ , the two remaining bands at ca. 3717 and 3671  $\text{cm}^{-1}$  shift progressively and respectively to 3687 and 3663  $\text{cm}^{-1}$ . So the 3 bands, which have disappeared in the hydroxyls region, are connected with the presence of the traces of sulfate, and the shift of the remaining hydroxyls groups indicates a protonation of  $\text{NH}_3$ , but it is so weak that  $\text{NH}_4^+$  is not detected. Moreover, the weak  $\nu(\text{S}=\text{O})$  vibration is affected by the  $\text{NH}_3$  adsorption by shifting to ca. 1331 and 1324  $\text{cm}^{-1}$  at the fifth and sixth aliquot respectively, then disappears from the seventh aliquot. It can be noticed that from the fourth aliquot a weak band started to appear at ca. 1330  $\text{cm}^{-1}$ , while the 1364  $\text{cm}^{-1}$  band started to decrease in intensity. In parallel, a new band appears at ca. 1046  $\text{cm}^{-1}$  at the fourth aliquot and shifts to ca. 1052  $\text{cm}^{-1}$  at the fifth aliquot and to ca. 1057  $\text{cm}^{-1}$  at the sixth aliquot. These latter bands are associated with the 1331 and 1324  $\text{cm}^{-1}$  and correspond, respectively, to  $\nu_{\text{S-O}}$  and  $\nu_{\text{S=O}}$  sulfuryls bands assigned to very few isolated surface  $[\text{SO}_4]^{2-}$  groups;<sup>8,14</sup> we assign this couple of bands to the monosulfate species. All these linked bands disappeared after the sixth aliquot. The band at initially ca. 1165  $\text{cm}^{-1}$  shifted progressively to 1153  $\text{cm}^{-1}$  at the seventh aliquot, then after saturation with  $\text{NH}_3$ , the band was centered at ca. 1161  $\text{cm}^{-1}$ .

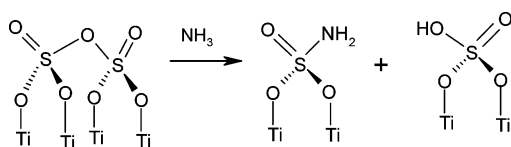
After final evacuation, however, a new band appeared at ca. 1297  $\text{cm}^{-1}$ , that we assigned to a new acid site where ammonia was physisorbed; this band can be associated with a new band at ca. 3570  $\text{cm}^{-1}$ , which may be a new Brönsted acid site, attributed a hydroxyl vibration associated with the monosulfate species; therefore, these two bands at ca. 1297 and 3570  $\text{cm}^{-1}$  are associated with monosulfate species. We can then assume that the very low quantity of acidic sites, which reacted with  $\text{NH}_3$ , are transformed to weaker acidic sites, even if their characteristic vibrations are very weak in the IR spectrum, as seen by their very low absorbance intensity.

## Discussion

The original oxides are basic as illustrated in Figure 1. Indeed, the basicity of GP350 is comparable to that of  $\text{KF}/\gamma\text{-Al}_2\text{O}_3$ , which is a well-known base,<sup>31,32</sup> adsorbing  $\text{CO}_2$  with an initial enthalpy of adsorption of about 110 kJ/mol.<sup>33</sup> DT51 contains sulfates due to its synthesis and shows a lower basic strength due to the inhibition of the basic sites by sulfates. The effect of the structure of titania appears when comparing anatase with rutile. Earlier works reported anatase as amphoteric and rutile as basic;<sup>34</sup> however, for the adsorption of  $\text{CO}_2$ , anatase shows a higher basicity.

Sulfuric acid is much more acidic than  $\text{CO}_2$ , and the number of S atoms retained by the solid is about 5–10 times the number of  $\text{CO}_2$  molecules (Figure 2). The density of sulfates trapped by the solid is much higher on P25, about 15  $\mu\text{mol}/\text{m}^2$  compared to 1.7 on GP350. The selectivity of P25 for sulfates is surprisingly high, and if we accept that basic sites are defects in the solid, this would imply that the surface of P25 indeed contains many defects.

Sulfates are well-known to block sintering of zirconias and titanias so that the surface areas of the sulfated materials remains in the range of 90–100  $\text{m}^2/\text{g}$  after treatment at 773K, whereas non sulfated materials sinter heavily (Table 1). A treatment above 873 K decomposes the sulfates and induces a more severe

**SCHEME 1: Interaction of Ammonia with the Disulfate**

sintering. It is interesting to observe that the stability of sulfates also depends on the support, and that P25 loses its sulfates easier than GP350 upon calcination at 773 K. The different stability suggests that the structures could be different. Another argument can be found in the comparison of the spectra of the sulfates formed here with those recently reported for sulfated titanias obtained by sol gel using sulfuric acid.<sup>35</sup> In both cases, the solid was dehydroxylated after calcination at 773K, and the main difference lies in the relative intensities of the bands at 1385 and 1111  $\text{cm}^{-1}$ ; the sol gel samples show bands of similar intensities, while we observe here a weak band at 1111  $\text{cm}^{-1}$ , suggesting that the structure of sulfates is quite different. It has to be pointed out that the band at 1385  $\text{cm}^{-1}$  appears only at the higher S contents (Figure 5), and is more intense on the solid of higher surface area. Another clear result is that sulfates differently promote acidity of the different titanias; a clear increase of the density of acid sites is observed only for GP350. The other titanias show little change of the number of acid sites per  $\text{m}^2$ . The particularity of GP350 is a higher surface area, which suggests that the acid sites are sulfates linked to Ti atoms of low coordination, in good agreement with quantum calculations performed in the case of zirconia.<sup>36</sup>

The calorimetric study of the interaction of ammonia with sulfated titania shows a lack of signal for the first increments, despite a significant adsorption of  $\text{NH}_3$ . This phenomenon has been observed only for the sulfated materials, and has been reported earlier for sulfated aluminas.<sup>37</sup> It is, therefore, attributed to an interaction of ammonia with the sulfates. This interaction can be more precisely investigated by infrared spectrometry introducing small doses of ammonia. This study shows that  $\text{NH}_3$  is dissociated on sulfated titania, with formation of new OH species, of lower acidity. In this process, the band at 1400  $\text{cm}^{-1}$  attributed to disulfates disappears and the bands of mono sulfates grow. The infrared data could be summarized by a simple reaction, described in Scheme 1, in which the disulfate is decomposed by ammonia, leaving an S—OH which can react further to give  $\text{NH}_4^+$  and, therefore, lead to the formation of  $\text{NH}_4\text{HSO}_4$ . The very low initial enthalpy of adsorption observed by calorimetry on sulfated titanias supposes the occurrence of an endothermic process counterbalancing the exothermic process of adsorption. The dissociation of  $\text{NH}_3$  is endothermic, and this reaction is consistent with both types of results.

The adsorption of  $\text{NH}_3$  is then a complex process in that case. If we assume that the sites which dissociate  $\text{NH}_3$  are disulfates, their number can be estimated from the thermogram and corresponds to about 7% of the sites adsorbing  $\text{NH}_3$ , therefore a small fraction of the acid sites. The number of strong acid sites able to crack paraffins has also been reported to be a small fraction of the total number of sites.<sup>38</sup>

**Conclusions**

The acid properties of sulfated titanias are relatively different according to the method used for their determination. The dissociation of  $\text{NH}_3$  at the surface, and its reaction with the disulfate groups has been evidenced by infrared spectrometry and accounts for an unusual calorimetric behavior restricted to sulfates. The number of acid sites and the stability of sulfates are controlled by the surface area of the initial support, which

may explain that large discrepancies exist in the literature of the acidity of this class of catalysts. IR spectroscopy is a powerful tool to probe the interaction of strong bases with titanium oxide samples by probing the Brønsted acidity of hydroxyls groups for both samples, and showing the transformation of disulfate species to monosulfate species on a sulfated titanium dioxide sample.

**Supporting Information Available:** Tables of the bands and their assignments for different increments of  $\text{NH}_3$  introduced onto the solids. This material is available free of charge via the Internet at <http://pubs.acs.org>.

**References and Notes**

- (1) Hino, M.; Arata, K. *Chem. Commun.* **1979**, 1148.
- (2) Arata, K.; Matsushashi, H.; Hino, M.; Nakamura, H. *Catal. Today* **2003**, *81*, 17.
- (3) Rajadhyaksha, R. A.; Chaudhari, D. D. *Ind. Eng. Chem. Res.* **1987**, *26*, 1743.
- (4) dos Santos, A. C. B.; Kover, W. B.; Faro, A. C., Jr. *Appl. Catal., A* **1997**, *153*, 83.
- (5) Bolis, V.; Magnacca, G.; Cerrato, G.; Morterra, C. *Langmuir* **1997**, *13*, 888.
- (6) Bensitel, M.; Saur, O.; Lavalley, J. C.; Mabilon, G. *Mater. Chem. Phys.* **1987**, *17*, 249.
- (7) Bensitel, M.; Saur, O.; Lavalley, J. C.; Morrow, B. A. *Mater. Chem. Phys.* **1988**, *19*, 147.
- (8) Morterra, C.; Cerrato, G.; Emanuel, C.; Bolis, V. *J. Catal.* **1993**, *142*, 349.
- (9) Morterra, C.; Cerrato, G.; Bolis, V. *Catal. Today* **1993**, *17*, 505.
- (10) Escalona Platero, E.; Penarroya Mentruit, M.; Otero Arean, C.; Zecchina, A. *J. Catal.* **1996**, *162*, 268.
- (11) Yamaguchi, T.; Jin, T.; Tanabe, K. *J. Phys. Chem.* **1986**, *90*, 3148.
- (12) Jin, T.; Yamaguchi, T.; Tanabe, K. *J. Phys. Chem.* **1986**, *90*, 4794.
- (13) Hino, M.; Arata, K. *Chem. Commun.* **1980**, 851.
- (14) Chen F. R.; Coudurier, G.; Joly, J. F.; Vedrine, J. C. *J. Catal.* **1993**, *143*, 616.
- (15) Bolis, V.; Magnacca, G.; Cerrato, G.; Morterra, C. *Thermochim. Acta* **2001**, *379*, 147.
- (16) Morterra, C.; Cerrato, G.; Meligrana, G.; Signoretto, M.; Pinna, F.; Strukul, G. *Catal. Lett.* **2001**, *73*, 113.
- (17) Biro, K.; Figueras, F.; Alvarez, C. M.; Bekassy, S.; Valyon, J. *J. Therm. Anal. Calorim.* **1999**, *56*, 345.
- (18) Biro, K.; Figueras, F.; Bekassy, S. *Appl. Catal., A* **2002**, *229*, 235.
- (19) Xia, Y. D.; Hua, W. M.; Tang, Y.; Gao, Z. *Chem. Commun.* **1999**, 1899–1900.
- (20) Xu, B.-Q.; Sachtler, W. M. H. *J. Catal.* **1997**, *167*, 224.
- (21) Gonzalez, M. R.; Kobe, J. M.; Fogash, K. B.; Dumesic, J. A. *J. Catal.* **1996**, *160*, 290.
- (22) Quaschnig, V.; Deutsch, J.; Druska, P.; Niclas, H.-J.; Kemnitz, E. *J. Catal.* **1998**, *177*, 164.
- (23) Rosenberg, D. J.; Anderson, J. A. *Catal. Lett.* **2002**, *83*, 59.
- (24) Tsyganenko, A. A.; Pozdnyakov, D. V.; Filimonov, V. N. *J. Mol. Struct.* **1975**, *29*, 299.
- (25) Bodoardo, S.; Figueras, F.; Garrone, E. *J. Catal.* **1994**, *147*, 223.
- (26) Lonyi, F.; Valyon, J.; Engelhardt, J.; Mizukami, F. *J. Catal.* **1996**, *160*, 279.
- (27) Sohn, J. R.; Kim, H. W. *J. Mol. Catal.* **1989**, *52*, 361.
- (28) Morterra, C.; Cerrato, G.; Pinna, F.; Signoretto, M. *J. Catal.* **1995**, *157*, 109.
- (29) Socrates, G. *Infrared and Raman characteristic group frequencies*; J. Wiley & Sons: New York, 2001.
- (30) Busca, G.; Saussey, H.; Saur, O.; Lavalley, J. C.; Lorenzelli, V. *Appl. Catal.* **1985**, *14*, 245.
- (31) Duke, C. V. A.; Miller, J. M.; Clark, J. H.; Kybett, A. P. *J. Mol. Catal.* **1990**, *62*, 233.
- (32) Ando, T.; Clark, J. H.; Cork, D. G.; Hanafusa, T.; Ichihara, J.; Kimura, T. *Tetrahedron Lett.* **1987**, *28*, 1421.
- (33) Clacens, J.-M.; Genuit, D.; Delmotte, L.; Garcia-Ruiz, A.; Bergeret, G.; Montiel, R.; Lopez, J.; Figueras, F. *J. Catal.* **2004**, *221*, 483.
- (34) Mathieu, M. V.; Primet, M.; Pichat, P. *J. Phys. Chem.* **1971**, *75*, 1221.
- (35) Bokhim, X.; Morales, A.; Ortíz, E.; López, T.; Gómez, R.; Navarrete, J. *J. Sol-Gel Sci. Technol.* **2004**, *29*, 31.
- (36) Kanougi, T.; Atoguchi, T.; Yao, S. *J. Mol. Catal., A* **2002**, *177*, 289.
- (37) Gervasini, A.; Fenyesi, J.; Auroux, A. *Langmuir* **1996**, *12*, 5356.
- (38) Marcus, R. L.; Gonzalez, R. D.; Kugler, E. L.; Auroux, A. *Chem. Eng. Commun.* **2003**, *190*, 1601.